University of Groningen

Versatile Coordination Behaviour of Cyclopentadienyl-Arene Ligands on Early Transition Metals

Otten, Edwin

IMPORTANT NOTE: You are advised to consult the publisher's version (publisher's PDF) if you wish to cite from it. Please check the document version below.

Document Version
Publisher's PDF, also known as Version of record

Publication date:
2008

Link to publication in University of Groningen/UMCG research database

Citation for published version (APA):
Otten, E. (2008). *Versatile Coordination Behaviour of Cyclopentadienyl-Arene Ligands on Early Transition Metals*. [Thesis fully internal (DIV), University of Groningen]. University of Groningen.

Copyright
Other than for strictly personal use, it is not permitted to download or to forward/distribute the text or part of it without the consent of the author(s) and/or copyright holder(s), unless the work is under an open content license (like Creative Commons).

The publication may also be distributed here under the terms of Article 25fa of the Dutch Copyright Act, indicated by the "Taverne" license. More information can be found on the University of Groningen website: https://www.rug.nl/library/open-access/self-archiving-pure/taverne-amendment.

Take-down policy
If you believe that this document breaches copyright please contact us providing details, and we will remove access to the work immediately and investigate your claim.

Downloaded from the University of Groningen/UMCG research database (Pure): http://www.rug.nl/research/portal. For technical reasons the number of authors shown on this cover page is limited to 10 maximum.

Download date: 06-05-2023

Chapter 4 'Low-valent' complexes of titanium with *ansa*-Cp-arene ligands

A key intermediate in ethylene trimerisation catalysed by cyclopentadienyl-arene titanium complexes is a low-valent titanium(II) species.[1-3] The coordination of the pendant arene moiety is presumed to provide additional stabilisation to this highly reactive species. Indeed, group 4 metal complexes in their +2 oxidation state are rare and highly reactive.[4,5] As an example, the parent titanocene, Cp_2Ti, has been long sought after, but never isolated due to its extreme reactivity.[6] The metal centre in titanocene(II) species may be stabilised by coordination of π-acidic ligands (e.g., CO, phosphine, ethylene, butadiene, acetylene) to give complexes with a bent metallocene structure (**A**). Introduction of sterically more demanding cyclopentadienyl derivatives has allowed the structural characterisation of linear titanocenes without additional ligands (Chart 4.1, **B**).[7,8] Taking advantage of the highly reducing nature of low-valent metallocenes, coordination of dinitrogen to these metal centres has been achieved. Recently, Chirik and co-workers showed that, upon coordination to a homogeneous zirconocene(II) complex, hydrogenation and cleavage of dinitrogen is feasible.[9] This elusive transformation is facilitated by the side-on coordination of the N_2 ligand.[10] Although several end-on bound titanocene N_2 dimers are known, only very recently side-on coordination to titanium was realised (**C**).[11] With the recent discovery of a monomeric bis(dinitrogen) titanocene complex,[11] as well as related mono(dinitrogen) and CO adducts (**D**),[12] the family of well-characterised low-valent group 4 metal complexes has been substantially expanded.

Chart 4.1

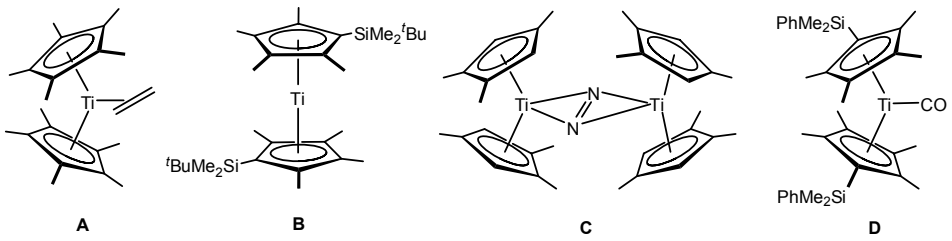

A **B** **C** **D**

In Chapter 3, we established computationally the isolobal relationship between the *ansa*-Cp-arene titanium fragment and its metallocene counterpart. Based on this, we anticipated that *ansa*-Cp-arene titanium(II) compounds analogous to titanocene(II) might be accessible. This chapter provides a combined experimental and computational study on the role of the pendant arene moiety in stabilising these types of *ansa*-Cp-arene complexes of titanium(II).

4.1. SYNTHESIS OF *ANSA*-CP-ARENE TITANIUM(II) CATIONS

4.1.1. Attempted preparation of half-sandwich Cp-arene titanium butadiene complexes

Given the literature examples of isolable titanocene(II) complexes stabilised by π-acidic ligands, we decided to investigate the accessibility of the analogous *ansa*-Cp-arene complexes. Our initial focus was on the synthesis of Cp-arene complexes of titanium with butadiene ligands. It is known that butadiene ligands are well-suited to stabilise early transition metal complexes in low oxidation states. This can be attributed to the fact that the binding of the butadiene ligand lies in between the limiting σ^2,π (metalacyclopentene) and π,η^4 (diene) resonance contributions (Scheme 4.1). The σ^2,π structure is related to the π,η^4 mode by oxidative addition to the metal centre, with concomitant reduction of the diene to a but-2-ene-1,4-diyl dianion. For the half-sandwich complex Cp^*Ti(butadiene)Cl, spectroscopic and structural features indicate substantial π,η^4 character in the binding of the butadiene ligand, whereas heavier group 4 congeners seem to favour σ^2,π coordination.[13-15]

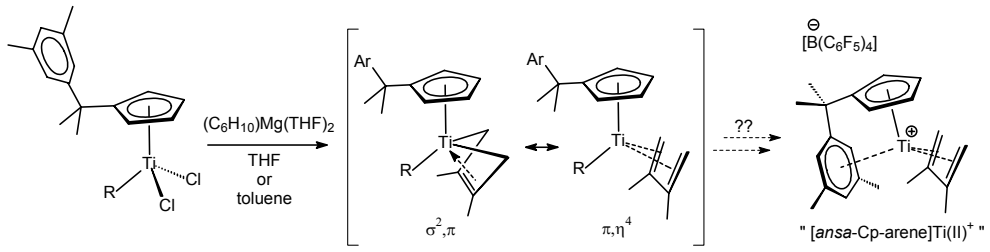

Scheme 4.1. Attempted synthesis of titanium butadiene complexes with Cp-arene ligands.

The ability of butadiene ligands to stabilise low-valent early transition metal complexes was shown for the scandium 1,3-diene complex $[\eta^6{:}\eta^1\text{-}C_5H_4(CH_2)_2NMe_2]Sc$(diene) (diene = 2,3-dimethyl-1,3-butadiene) that serves as precursor for a Sc(I) fragment by liberation of the butadiene.[16] We anticipated that, in a similar way, cationic titanium compounds of the type [*ansa*-Cp-arene]Ti(diene)$^+$ might provide a general entry into the chemistry of [*ansa*-Cp-arene]Ti(II)$^+$ (Scheme 4.1).

Attempts to form the desired half-sandwich titanium complex [Ar-CMe_2-η^5-C_5H_4]Ti(diene)R (Ar = 3,5-Me_2Ph; R = Cl, Me; diene = 2,3-dimethyl-1,3-butadiene) by reaction of [Ar-CMe_2-η^5-C_5H_4]$TiCl_2$R with (diene)Mg·$(THF)_2$ at -50 ºC in THF or toluene resulted, after slow warming to room temperature and extraction with pentane, in a black tar. ^{1}H NMR analysis of the crude reaction mixtures indicated the presence of the desired compounds, as seen e.g. from the characteristic doublets of the diene methylene *syn* and *anti* protons (for R = Me) at δ 2.82 and 0.99 ppm, respectively, with $^2J_{HH}$ of 8.4 Hz (Scheme 4.1). On the basis of ^{1}H NMR integration of these complexes versus the residual

solvent peak it seems, however, that the majority of the species in solution is paramagnetic. We were unable to improve the reaction conditions and obtain the titanium butadiene complexes in pure form. It should be noted that, although $Cp^*Ti(diene)Cl$ can be prepared using this procedure in ca. 40-60% yield,[14] analogous complexes that lack substituents on the cyclopentadienyl moiety are absent from the literature. We therefore tentatively conclude that the mono-substituted cyclopentadienyl ligands used here do not provide sufficient steric protection to impart reasonable stability to the intermediate(s) that are formed during synthesis of the complex.

Examples of other monocyclopentadienyl group 4 metal complexes in their +2 oxidation state with ligands other than butadiene are exceedingly rare. Ellis and co-workers described the synthesis of $Cp^*M(CO)_2(dmpe)Cl$ (M = Ti, Zr, Hf; dmpe = $Me_2PCH_2CH_2PMe_2$).[17] The stability of these was shown to dramatically decrease in the order Hf > Zr > Ti, such that for M = Hf the complex could be isolated and crystallographically characterised, whereas attempts to isolate the titanium analogue led to extensive decomposition. Similar complexes with unsubstituted cyclopentadienyl ligands have also been reported, but also in this case the titanium derivative could not be prepared.[18] A few examples of half-sandwhich titanium(II) complexes of the type CpTiR(dmpe) (R = Cl, Me, H) have been reported, but their chemistry has not been studied extensively.[19] In addition, the titanium(II) compounds $TiCl_2(tmeda)_2$ (tmeda = $Me_2NCH_2CH_2NMe_2$),[20] $TiCl_2(pyridine)_4$,[21] and $TiMe_2(dmpe)_2$[22] have been synthesised and structurally characterised. Although these compounds could be regarded as convenient starting materials for derivatisation (e.g., by salt metathesis or alkane elimination methodology), no examples of such transformations exist in the literature. Our attempts to react $TiCl_2(tmeda)_2$ with [Ar-CMe_2-C_5H_4]Li or Ar-CMe_2-$C_5H_4SiMe_3$ to generate "[Ar-CMe_2-C_5H_4]TiCl$(tmeda)_x$" invariably led to intractable black reaction mixtures, probably due to decomposition of the starting material: the low solution stability of $TiCl_2(tmeda)_2$ has been noted previously.[20]

4.1.2. Synthesis of 'low-valent' *ansa*-Cp-arene titanium complexes with carbonyl ligands

Based on the isolobal relationship between the *ansa*-Cp-arene titanium cations described in Chapters 2 and 3 and their neutral metallocene analogues, we felt that low-valent *ansa*-Cp-arene titanium(II) species may be accessible starting from a complex in which the *ansa*-coordination is already present. The synthesis of a large portion of characterised titanocene(II) complexes involves the reduction of a titanocene(IV) halide of the type Cp_2TiX_2 (X = Cl, Br, I) with strong reductants (e.g., Na/Hg) in the presence of a suitable ligand, such as CO, acetylene, etc.[23,24] A similar approach to generate the corresponding *ansa*-Cp-arene titanium(II) cations would be extremely challenging, since it would require a soluble, cationic *ansa*-Cp-arene titanium halide species of the type [*ansa*-Cp-arene]TiX_2^+. Clearly, the solvents that are typically used to dissolve such ionic species (bromobenzene, dichloromethane) are incompatible with the strong reductants that are required to reach the +2 oxidation state for titanium.

Alternatively, the titanocene(II) complex $Cp_2Ti(CO)_2$ has been prepared starting from titanocene dialkyl compounds.[25] Brintzinger and co-workers found that treatment of Cp'_2TiMe_2 (Cp' = Cp, Cp^*) with H_2 gives the dimeric compounds $(Cp'_2TiH)_2$ or $(Cp'_2Ti)_2$, depending on the reaction conditions, which both rapidly react with CO to give good yields of the titanocene dicarbonyl.[26,27] Floriani and co-workers have reported that $Cp_2Ti(CO)_2$ is generated by carbonylation of $Cp_2Ti(CH_2Ph)_2$ under mild conditions. Based on the observation of dibenzylketone as a reaction product, an acyl intermediate was postulated.[28] Also Cp_2TiMe_2 is conveniently converted to $Cp_2Ti(CO)_2$ *via* an acyl species upon treatment with CO, with concomitant formation of acetone.[29,30]

Along similar lines, the reaction of the titanium(IV) dimethyl cation **3b** with CO results in the formation of the cationic dicarbonyl species $\{[\eta^6\text{-Ar-CMe}_2\text{-}\eta^5\text{-C}_5\text{H}_4]\text{Ti(CO)}_2\}[\text{B(C}_6\text{F}_5)_4]$ (**5b**) (Scheme 4.2). Monitoring the reaction of **3b** with 1 bar of CO in C_5D_5Br solution by ^1H NMR spectroscopy shows full consumption of the starting material within 10 minutes. Although the reaction is not clean, the dicarbonyl species is the major product (the side products have not been identified). Complex **5b** precipitates as red crystals from the C_6D_5Br solution upon standing at room temperature overnight. Alternatively, and with higher yield, **5b** is prepared by treatment of solid **3b** with excess CO. The orange colour of the starting material gradually darkens to red in the course of 3 days and ^1H NMR analysis of the crude reaction mixture indicates a greater purity compared to the analogous reaction in solution.

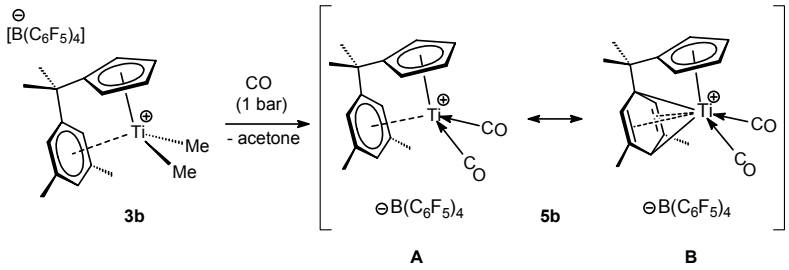

Scheme 4.2. Synthesis of $\{[\eta^6\text{-Ar-CMe}_2\text{-}\eta^5\text{-C}_5\text{H}_4]\text{Ti(CO)}_2\}[\text{B(C}_6\text{F}_5)_4]$ (**5b**).

To determine the fate of the Ti-Me groups in **3b**, wet C_6D_5Br was added to an NMR tube containing the crude reaction mixture of the reaction of solid **3b** with CO (see Experimental Section for details). The ^1H NMR spectrum taken immediately after mixing showed the presence of **5b** and acetone (δ 1.81 ppm). When dry C_6D_5Br is added or when the reaction is carried out in dry C_6D_5Br solution, no acetone is observed. We propose that the acetone that is formed reacts with either starting material or product to give an unknown (paramagnetic) species, hydrolysis of which liberates acetone. It thus appears that the reactivity of the *ansa*-Cp-arene titanium dimethyl cation towards CO follows a pathway that is analogous to that found in the carbonylation of dialkyl metallocenes of the group 4 triad.[25,28,30,31]

The ^{1}H NMR spectrum of **5b** in C_6D_5Br is consistent with a C_s symmetric compound, and shows resonances for the arene moiety at δ 5.00 (*p*-H) and 4.38 ppm (*o*-H). The corresponding signals in **3b** are found at δ 7.02 and 5.91 ppm, respectively.[32] The upfield shift for the arene resonances suggests (at least partial) reduction of the arene ring in **5b**. Also, in the ^{13}C NMR spectrum the resonances for the C_6 ring are located significantly upfield from the aromatic region (δ 102.6/100.3/86.8 ppm for C_{ortho}/C_{para}/C_{ipso}). The crystal structure of **5b** (Figure 4.1, pertinent interatomic distances and bond angles in Table 4.1) also shows an *ansa*-Cp-arene geometry, related to **3b**. But in marked contrast to the titanium(IV) dimethyl cations like **3b** and others described in Chapter 2, the Ti-C_{para} bond (2.395(4) Å) is *shorter* than the Ti-C_{meta} distances (av. 2.472 Å), and the C_6 ring is not planar, with folding along the C(19)-C(112) axis of 10.2(3)°. In addition, the C_{ortho}-C_{meta} distances in the ring are noticeably shorter (1.387(6) and 1.396(6) Å for C(110)-C(111) and C(113)-C(114), respectively) than the other C-C bonds (av. 1.419 Å), which indicates a considerable degree of π-localisation in the C_6 ring (Table 4.2). Taken together, these data are indicative of contribution of the Ti(IV)/dienediyl resonance structure depicted in Scheme 4.2 (structure **B**).

A few related 'unbrigded' arene complexes of group 4 metals have been reported and show substantially larger fold angles in the range of 20-30°.[33-36] Stephan and co-workers have shown that Mg reduction of the phosphinimide complexes Cp'Ti[NP^{t}Bu$_2$(2-biphenyl)] (Cp' = Cp, Cp*) results in complexes that coordinate the pendant arene ring of the biphenyl substituent. In these compounds, the fold angle (25.3-25.9°) is consistent with a Ti(IV)/reduced arene formulation.[37] The strained *ansa*-Cp-arene coordination in **5b** (evident from the very acute C(15)-C(16)-C(19) angle of 94.3(3)º) precludes optimal overlap between metal d- and arene π^*-orbitals. Consequently, the degree of reduction of the arene is lower than that of titanium(II) species without strained arene coordination.

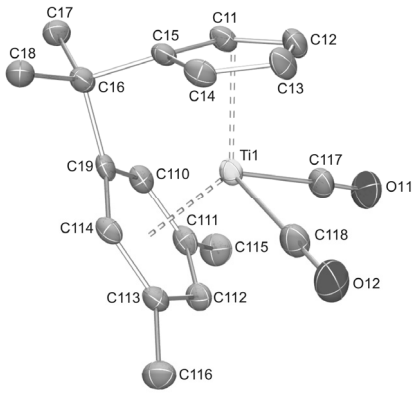

Figure 4.1. Molecular structure of **5b** showing 50% probability ellipsoids. The $B(C_6F_5)_4$ anion and hydrogen atoms are omitted for clarity.

Table 4.1. Selected bond distances (Å) and angles (º) for **5b**.

Ti(1)–C(117)	2.091(5)	C(117)–O(11)	1.135(5)
Ti(1)–C(118)	2.100(5)	C(118)–O(12)	1.129(6)
Ti(1)–Cg(Cp)	1.994(2)	Ti(1)–Cg(Ar)	1.9341(16)
Ti(1)–C(11)	2.291(5)	Ti(1)–C(19)	2.264(4)
Ti(1)–C(12)	2.382(4)	Ti(1)–C(110)	2.372(4)
Ti(1)–C(13)	2.391(4)	Ti(1)–C(111)	2.466(3)
Ti(1)–C(14)	2.299(5)	Ti(1)–C(112)	2.395(4)
Ti(1)–C(15)	2.270(3)	Ti(1)–C(113)	2.478(4)
C(15)–C(16)–C(19)	94.3(3)	Ti(1)–C(114)	2.373(4)
Cg(Cp)–Ti(1)–Cg(Ar)	130.60(8)	α^a	57.6(3)
$\phi_{Cp}{}^b$	15.3(3)	$\phi_{Ar}{}^b$	21.8(2)
$\tau_{Cp}{}^c$	4.2(2)	$\tau_{Ar}{}^c$	3.99(13)

[a] α is the interplanar angle between the least-squares planes of the cyclopentadienyl and arene rings. [b] ϕ_{Cp} / ϕ_{Cp} is the angle between the C_{ipso}-C(16) vector and the least-squares planes of the cyclopentadienyl / arene rings, respectively. [c] τ_{Cp} / τ_{Ar} is the angle between the Ti(1)-Cg(Cp) / Ti(1)-Cg(Ar) vector, respectively, and the ring normal. See also Chapter 2, Figure 2.2.

Table 4.2. Comparison of experimental and calculated arene C-C bond distances (Å) and arene folding (º) in *ansa*-Cp-arene cations with C_1 bridge.

	3b	**3b'** [b]	**5b**	**5b'** [c]
$C_{ipso} - C_{ortho}$	1.409(5)	1.409	1.425(4)	1.425
	1.410(5)	1.408	1.421(7)	1.425
$C_{ortho} - C_{meta}$	1.402(5)	1.409	1.387(6)	1.399
	1.414(5)	1.409	1.396(6)	1.399
$C_{meta} - C_{para}$	1.383(5)	1.400	1.419(7)	1.420
	1.380(5)	1.399	1.412(4)	1.420
ring folding[a]	0.3(3)	1.19	10.2(3)	11.58

[a] folding along the C(19) – C(112) axis. [b] DFT optimised geometry; see Chapter 3. [c] DFT optimised geometry; see section 4.2.

For the carbonyl ligands in **5b**, the crystallographic C-O bond lengths (1.129(6) and 1.135(5) Å) are virtually identical, and Ti-C(carbonyl) distances (2.091(5) and 2.100(5) Å) are marginally longer compared to the corresponding distances for CO ligands in typical Ti(II) systems (e.g., $Me_2Si(C_5Me_4)_2Ti(CO)_2$, C-O: 1.134(9) and 1.129(11) Å; Ti-C(carbonyl): 2.017(8) and 2.040(9) Å).[38] In the ^{13}C NMR spectrum of **5b**, the signal for the CO ligands is observed at δ 227.3 ppm. This is intermediate between the ^{13}C NMR resonances of the carbonyl groups in d^2 titanocenes ($Cp_2Ti(CO)_2$: δ 260.5 ppm)[39] and free CO (δ 184.5 ppm in toluene-d_8 solution),[40] and compares well with d^0 group 4 metal CO adducts (e.g., $Cp_2Zr(C_3H_5)(CO)^+$: δ 218.7 ppm).[41] In the IR spectrum of **5b** two bands are observed at 2055 and 2022 cm^{-1} for the symmetric and anti-symmetric CO stretching vibrations, respectively. Although lower than free CO (2143 cm^{-1}), these values are significantly higher than those found for typical d^2 titanocenes (Table 4.3). Conversely, stable d^0 metal complexes with CO ligands are rare, due to the lack of stabilising metal→CO π-backbonding interactions.[42,43] In cases when isolable adducts are formed, these are usually stabilised by donation from a metal–ligand σ-orbital into the CO π^*-orbital ($\sigma \rightarrow \pi^*$ backbonding).[41,44-51] A comparison of representative group 4 metal carbonyl adducts is collected in Table 4.3, showing that, in agreement with the structural features of the coordinated arene, compound **5b** is best described by significant contribution of resonance structure **B** (Scheme 4.2).[52]

Table 4.3. Infrared frequencies of CO ligands representative group 4 metal complexes.

	υ(CO) (cm^{-1})	$\upsilon(CO)_{av}$ (cm^{-1})	ref
$Cp_2Ti(CO)_2$	1977, 1899	1938	53
$Me_2Si(C_5H_4)_2Ti(CO)_2$	1980, 1905	1942.5	54
$Cp_2TiCl(CO)$		2068	55
$[Cp^*_2Zr(C_3H_5)(CO)]^+$		2079	41
$[Cp_3Zr(CO)]^+$		2132 / 2150	56,57
$[Cp_2Ti(CO)_2]^{2+}$	2119, 2099	2109	57,58
$Cp^*_2ZrH_2(CO)$		2044	45
5b	2055, 2022	2039	this work

A preliminary screening of the reactivity of **5b** was performed. Specifically, given the analogy with the low-valent intermediates in the ethylene trimerisation cycle, we were interested in its reactivity towards ethylene. On NMR scale, a solution of **5b** in C_6D_5Br solution was pressurised with 1 bar of ethylene. No reaction was observed at room temperature, whereas warming to 50 ºC slowly precipitated a purple solid. The product dissolves in THF-d_8, and is shown by ^1H NMR spectroscopy to be paramagnetic. The ionic

nature of the compound is confirmed by the signals of the $B(C_6F_5)_4$ anion in the ^{19}F NMR spectrum. No CO absorption bands are observed in the infrared spectrum, and we have not been able to clarify the nature of this purple product. Thermolysis of **5b** in the absence of ethylene also gave a purple precipitate. It thus appears that ethylene is not involved in the reactivity, and we tentatively conclude that ethylene is unable to displace the carbonyl ligands in **5b**. Dissociation of CO from transition metal compounds can be achieved by photochemical means. However, irradiation of a solution of **5b** using a Hg-lamp in the presence of 1 bar of ethylene also failed to initiate trimerisation.

4.1.3. Ligand effects in *ansa*-Cp-arene titanium dicarbonyls

In Chapters 2 and 3 we explored the effect of modifications of the Cp-arene ligand in titanium(IV) dimethyl cations, and noted considerable differences in the geometry of intramolecular arene coordination and the strength of the metal-arene interaction. To elucidate the effect of such modifications on *ansa*-Cp-arene titanium(II) dicarbonyl cations, we have prepared a series of compounds that differ in the length of the bridge between the cyclopentadienyl and arene moiety, or the substitution pattern of either arene or cyclopentadienyl part (Scheme 4.3).

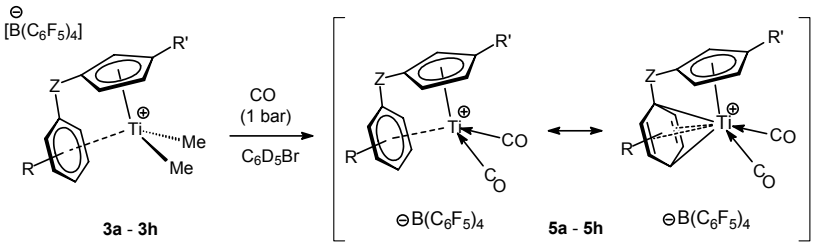

R = H; Z = CMe_2; R' = H (**a**)
R = 3,5-Me_2; Z = CMe_2; R' = H (**b**)
R = 3,5-Me_2; Z = CH_2CMe_2; R' = H (**c**)
R = H; Z = CMe_2; R' = $SiMe_3$ (**d**)
R = 3,5-Me_2; Z = CH_2; R' = $SiMe_3$ (**e**)
R = 3,5-Me_2; Z = CMe_2; R' = $SiMe_3$ (**f**)
R = 3,5-Me_2; Z = CH_2CMe_2; R' = $SiMe_3$ (**h**)

Scheme 4.3. Synthesis of cationic *ansa*-Cp-arene complexes of titanium(II) with carbonyl ligands.

For the synthesis of **5b** we found that the most convenient preparation involves treatment of **3b** in the solid state with 1 bar of CO (*vide supra*). The same procedure using solid **5c**, however, proceeded much more slowly, reaching ca. 35% conversion after a week at room temperature. In C_6D_5Br solution this reaction requires ca. 3 hours to go to completion (compared to < 10 min for **3b**), but as noted previously the product is generated less cleanly in solution. Unfortunately, regardless of the preparation procedure, the *ansa*-Cp-arene titanium dicarbonyl cations **5a,c-f**,**h** could not be crystallised, preventing isolation of the

complexes in analytically pure form. Therefore, these compounds were generated on NMR tube scale in C_6D_5Br solution and the crude products were characterised by NMR and IR spectroscopic methods. For each compound, ^{1}H NMR spectroscopy shows resonances of the coordinated arene moiety in the range of δ 5.5 – 4 ppm, indicative of partial reduction of the C_6 ring. As anticipated, the Me_3Si-substituted compounds **5d**-**f**,**h** are asymmetric and show two sets of signals for both the *ortho* and *meta* substituents of the C_6 ring. At room temperature, the sharp and inequivalent *ortho*-H resonances (**5f**: δ 4.41 and 4.38 ppm) indicate that arene exchange such as observed for **3f** is slow on the NMR timescale. Upon heating to 80 °C no line broadening is observed, from which we conclude that, in contrast to the titanium(IV) dimethyl cations described in Chapter 3, the Cp-arene ligands in the dicarbonyl compounds **5a**-**f**,**h** do no longer exhibit hemilabile behaviour. This is likely due to the partial reduction of the arene in these complexes, leading to a much stronger metal-arene interaction than for titanium(IV) complexes.

Table 4.4. Experimentally observed average ^{13}C NMR shift and infrared frequencies of CO ligands in **5a**-**f**,**h**.

	δ $(CO)_{av}$ (ppm)	υ(CO) (cm^{-1})	$\upsilon(CO)_{av}$ (cm^{-1})
5a	226.6	2064, 2032	2048
5b	227.3	2055, 2022	2039
5c	237.0	2039, 1997	2018
5d		2056, 2022	2039
5e	229.9	2047, 2010	2029
5f	229.2	2048, 2012	2030
5h	238.3	2033, 1989	2011
$Cp_2Ti(CO)_2$[a]	260.5	1977, 1899	1938

[a] ref 53

The infrared spectra obtained from the crude reaction mixtures of **5a**-**f**,**h** show only two bands in the region 1800-2200 cm^{-1} that are attributed to CO vibrations of the dicarbonyl cations. Apparently, other species that are present in the crude mixture do not contain terminal CO ligands, and a comparison of the IR frequencies is appropriate (Table 4.4). There is a significant decrease of ca. 20 cm^{-1} in the observed CO stretching frequency upon increasing the bridge length by one carbon atom (**5b** vs. **5c** and **5f** vs. **5h**). The increased electron-density in the arene ring by adding methyl substituents (Ph in **5a**/**d** vs. 1,3-Me_2Ph in **5b**/**f**) is seen to lower the average CO frequency by 9 cm^{-1}. A similar effect is observed for the $SiMe_3$-substituent on the cyclopentadienyl ring, which results in a lowering of $\upsilon(CO)_{av}$ by 7-9 cm^{-1} (compare, for instance, **5b** and **5f**). The latter is probably not related to

an inductive effect of the $SiMe_3$ group, since this is shown to be very small (ca. 1.5 cm^{-1}) in ziroconocene dicarbonyls.[59] Instead, the steric pressure exerted by the $SiMe_3$ group results in tilting of the cyclopentadienyl ring, which allows a closer approach of the arene moiety to the metal centre (see the crystal structure of **3f** in Chapter 2). Taken together, these results indicate that a pendant arene that is a better σ-donor results in a lowering of υ(CO). It thus appears that the σ-donor capacity of the pendant arene group is more important than its π-acceptor properties in modulating the electron density at the metal centre.

4.2. COMPUTATIONAL STUDIES ON *ANSA*-CP-ARENE TITANIUM(II) COMPLEXES

4.2.1. Optimised geometries and molecular orbital analysis

To obtain more insight in the nature of the *ansa*-Cp-arene coordination in the dicarbonyl complexes described above, we performed a series of DFT calculations. Because the crystal structure of **5b** is known (*vide supra*), we initially used this compound as a reference point to assess the accuracy of the DFT method in reproducing the structural details. The experimentally observed singlet ground state for **5b** is also obtained computationally: a triplet state with a nearly planar arene moiety is calculated to be 17.3 kcal·mol^{-1} higher in energy. The optimised structure (**5b'**) is in good agreement with that found by X-ray crystallography, with Ti-C(arene) distances that are only slightly longer by ~0.05 Å. Importantly, while the arene moiety in dimethyl cation **3b'** shows a fully delocalised π-system, the C-C bonds within the arene group of **5b'** manifest a similar degree of π-localisation as found in the X-ray structure (see Table 4.2); in addition, the ring is folded by 11.6° (X-ray structure: 10.2(3)°). The fact that DFT calculations accurately reproduce the experimentally obtained structure of **5b** led us to perform geometry optimisations on selected *ansa*-Cp-arene titanium dicarbonyl species described above for which no structural data are available. Metrical parameters and calculated IR absorption frequencies of the CO ligands in a series of representative *ansa*-Cp-arene titanium dicarbonyl cations are collected in Table 4.5. The corresponding values calculated for $Cp_2Ti(CO)_2$ using the same DFT method are included and substantially different from the *ansa*-Cp-arene cations, with shorter Ti-C(carbonyl) and longer C-O bond lengths, and υ(CO) shifted accordingly to lower wavenumbers. The calculated IR frequencies for the CO ligands in the *ansa*-Cp-arene titanium cations follow the experimentally observed trend.

Table 4.5. Calculated Ti-C(carbonyl) and C-O bond lengths (Å), and CO stretching frequencies for representative *ansa*-Cp-arene titanium dicarbonyl cations.

	$Ti\text{-}C(carbonyl)_{av}$	$C\text{-}O_{av}$	$\upsilon(CO)$ $(cm^{-1})^a$	$\upsilon(CO)_{av}$ $(cm^{-1})^a$
5a'	2.096	1.136	2071, 2045	2058
5b'	2.087	1.137	2061, 2034	2047
5c'	2.073	1.139	2048, 2016	2032
5d'	2.087	1.138	2061, 2032	2046
5f'	2.080	1.139	2020, 2051	2036
5h'	2.066	1.141	2004, 2038	2021
$Cp_2Ti(CO)_2$	2.039	1.150	1937, 1990	1964

[a] calculated frequencies after scaling by a factor of 0.97.[60,61]

To obtain a better understanding of the factors that govern the metal-arene interaction in these cationic titanium(II) systems, we performed geometry optimisations for the 'naked' cationic titanium(II) fragments $[\eta^6\text{-Ar-Z-}\eta^5\text{-}C_5H_4]Ti^+$ (Ar = 3,5-Me_2Ph; Z = CMe_2 (**Ti(b)**$^+$); Z = CH_2CMe_2 (**Ti(c)**$^+$)). A comparison between **Ti(b)**$^+$ and its titanium(IV) congener **Ti(b)**$^{3+}$ is given below (a similar analysis applies for **Ti(c)**$^+$). The overall geometries are the same for **Ti(b)**$^{3+}$/**Ti(b)**$^+$ and, as expected, the two additional electrons in **Ti(b)**$^+$ are located in the orbital that was the LUMO in **Ti(b)**$^{3+}$ (Figure 4.2.). The HOMO in **Ti(b)**$^+$ consists mainly of titanium based atomic orbitals (61%), indicating some Ti(II), d^2 character (Table 4.6). From the ligand, the major contribution to the HOMO involves the arene moiety (28%). The situation for the 'naked' titanium(IV) species **Ti(b)**$^{3+}$ is quite different, with the equivalent orbital (LUMO) being almost exclusively titanium-based (82%) with little contribution from the arene part (11%). The mixing of d-orbitals with the ligand orbitals that occurs on going from the *ansa*-Cp-arene titanium(IV) system **Ti(b)**$^{3+}$ to its titanium(II) derivative **Ti(b)**$^+$ is much less pronounced for the analogous *ansa*-titanocene system. The HOMO in $H_2C(\eta^5\text{-}C_5H_4)_2Ti$(II) has 72% Ti d-character, compared to 80% for its Ti(IV) congener. It thus appears that coordination of the pendant arene in **Ti(b)**$^+$ results in diminished d^2 character of the metal centre compared to $H_2C(\eta^5\text{-}C_5H_4)_2Ti$, due to delocalisation of d-electron density into the C_6-ring. Accordingly, the C_6 ring in **Ti(b)**$^+$ is folded (17.6º), while in **Ti(b)**$^{3+}$ it is essentially planar.

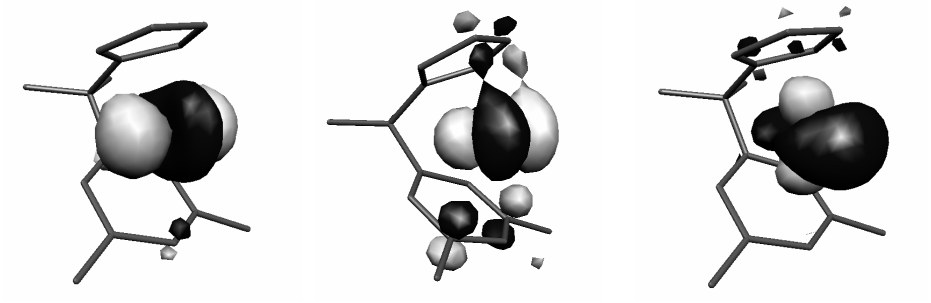

LUMO: -17.0 LUMO+1: -16.7 LUMO+2: -15.5

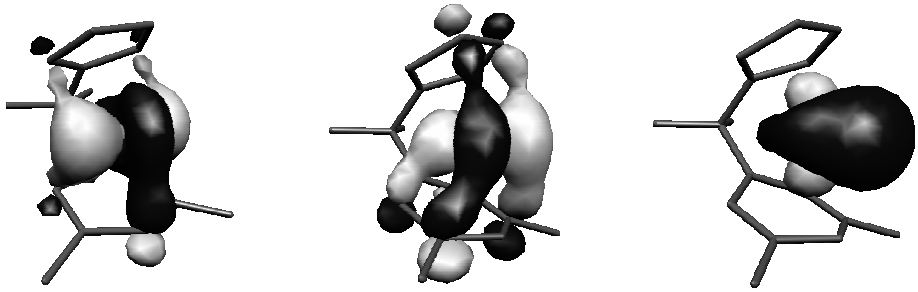

HOMO: -8.92 LUMO: -6.19 LUMO+1: -5.86

Figure 4.2. Frontier molecular orbitals of [η^6-Ar-CMe_2-η^5-C_5H_4]Ti^{3+} (**Ti(b)$^{3+}$**, top), [η^6-Ar-CMe_2-η^5-C_5H_4]Ti^{+} (**Ti(b)$^{+}$**, bottom), and their corresponding energies (eV).

Table 4.6. Percentage contributions of different fragments to the highest occupied molecular orbital in titanium(II) compounds (or the equivalent orbital (LUMO) in case of the titanium(IV) species **Ti(b)$^{3+}$** and $H_2C(\eta^5\text{-}C_5H_4)_2Ti^{2+}$).

	Ti	arene	Cp	$(CO)_2$
Ti(b)$^{3+}$	82	11	8	
Ti(b)$^{+}$	61	28	11	
$H_2C(\eta^5\text{-}C_5H_4)_2Ti^{2+}$	80	10	10	
$H_2C(\eta^5\text{-}C_5H_4)_2Ti$	72		14 + 13	
5b'	57	15	6	22
$H_2C(\eta^5\text{-}C_5H_4)_2Ti(CO)_2$	58		6 + 6	30

As was shown in Chapter 3 for the binding of two anionic σ-donor ligands (Me^-) to the fragment [η^6-Ar-CMe_2-η^5-C_5H_4]Ti^{3+}, the nature of the interaction between the two CO ligands and [η^6-Ar-CMe_2-η^5-C_5H_4]Ti^+ is analogous to that in the well-known neutral group 4 metallocene systems $Cp_2M(CO)_2$.[62,63] Analysis of the HOMO in the dicarbonyl cation **5b'** (Figure 4.3) shows that the main contributions are from orbitals on the metal centre (57%) and the CO ligands (22%), whereas the Cp-arene ligand is again involved mainly through the arene (15%). A comparison with the HOMO of the neutral *ansa*-titanocene analogue $H_2C(C_5H_4)_2Ti(CO)_2$[63] shows that for **5b'**, admixture of arene orbitals comes primarily at the expense of CO contribution (Table 4.6).

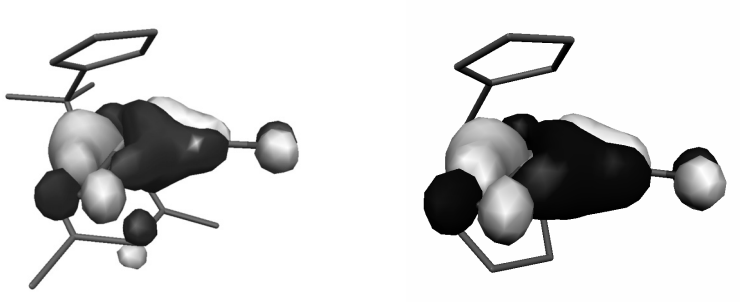

Figure 4.3. Highest occupied molecular orbital of the dicarbonyls [η^6-Ar-CMe_2-η^5-C_5H_4]$Ti(CO)_2^+$ (**5b'**, left) and $H_2C(\eta^5$-$C_5H_4)_2Ti(CO)_2$ (right).

4.2.2. Charge decomposition analysis

From the spectroscopic and structural data of the cationic dicarbonyl species **5b** it appears that there is some degree of reduction of the arene group, resulting in Ti(IV)/dienediyl character (Scheme 4.2, structure **B**). Such interactions may be described by the Dewar-Chatt-Duncanson model for coordination of π-conjugated ligands to a transition metal center[64,65] involving a combination of (*i*) donation from a filled ligand orbital into an empty orbital on the metal, and (*ii*) backdonation from an occupied metal d-orbital into an empty π^*-orbital of the ligand (see Chapter 3, Figure 3.4). Analysis of these donor-acceptor interactions was performed using the charge decomposition analysis (CDA) method developed by Frenking and co-workers, as described in Chapter 3.[66,67] This partitioning scheme has been applied in the analysis of the relative amount of metal→CO backdonation in a series of isoelectronic hexacarbonyl complexes (from $Hf(CO)_6^{2-}$ to $Ir(CO)_6^{3+}$), and it was shown to correlate with the CO stretching frequencies and C-O bond distances.[68,69] Here, we use this method to evaluate the relative amount of donation/backdonation for both the arene and the CO ligands in the *ansa*-Cp-arene dicarbonyl species described above. Fragments for the CDA analysis (Scheme 4.4) were obtained as described in Chapter 3.

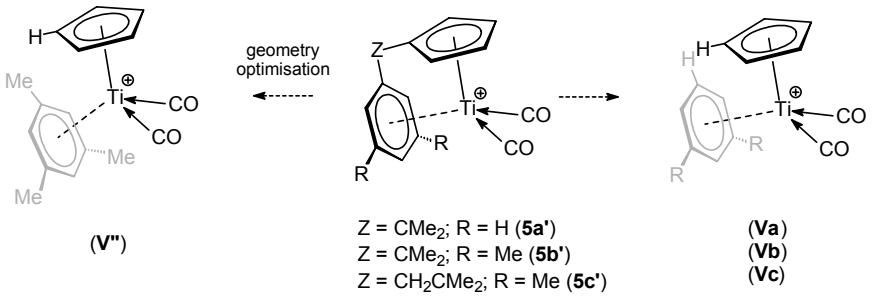

Scheme 4.4. Construction of arene and $CpTi(CO)_2^+$ fragments for the charge decomposition analysis.

The positive values for donation (*d*) and backdonation (*b*) together with the small residual term (Δ) obtained form the charge decomposition analysis (Table 4.7) indicate that the metal–arene interaction in all compounds is properly described by the Dewar-Chatt-Duncanson model.[67] In Chapter 3 it was shown that the interaction between the metal centre and the coordinated arene moiety in *ansa*-Cp-arene titanium(IV) cations results primarily from arene→Ti donation and backdonation is negligible, as anticipated for a d^0 metal centre. For the titanium(II) dicarbonyl cations studied here, a different situation arises due to the presence of d-electrons that are available for backdonation into the arene π^*-system. These compounds show a considerable amount of charge transfer due to backdonation, with *d*/*b* ratios around 4 (Table 4.7).

Table 4.7. Charge decomposition analysis of the metal-L interaction (L = arene, $(CO)_2$).

L = arene	*d* (e)	*b* (e)	*r* (e)	Δ (e)	*d*/*b*	E_b[a]
Ti(b)$^+$	0.739	0.243	-0.621	0.030	3.0	53.0
Ti(c)$^+$	0.788	0.256	-0.333	0.007	3.1	80.2
Va	0.771	0.182	-0.812	0.008	4.2	18.5
Vb	0.782	0.182	-0.760	-0.010	4.3	31.3
Vc	0.798	0.185	-0.409	-0.029	4.3	59.7
L = $(CO)_2$						
Va	0.844	0.310	-0.392	0.022	2.7	64.7
Vb	0.848	0.321	-0.402	0.024	2.6	65.5
Vc	0.874	0.353	-0.450	0.028	2.5	65.9
$Cp_2Ti(CO)_2$	0.918	0.476	-0.502	0.012	1.9	79.4

[a] the total bonding energy is the difference between the sum of the two fragments and the complex ($kcal \cdot mol^{-1}$)

Compared to the hypothetical 'naked' titanium(II) fragments **Ti(b)**$^+$, the Ti→arene backdonation in the dicarbonyl species **Vb** is reduced due to the presence of additional acceptor ligands (CO). A similar trend based on charge decomposition analysis has been observed for the metal–acetylene interaction in $M(CO)_4(C_2H_2)$ (M = Fe, Ru) and its CO dissociation product $M(CO)_3(C_2H_2)$.[70] The orbital that contributes mostly to the Ti→L backdonation is the same for both L = arene and CO, as illustrated for **Vb**/**c** in Figure 4.4, and thus the ligands are in competition for backdonation from the metal centre.

The influence of the ligand modifications on the Ti→arene backdonation *b* is relatively minor. The arene becomes only a slightly better acceptor when the strain in the *ansa*-coordination is alleviated by introducing a C_2 bridge (**Vb** vs. **Vc**). Changing the substituents on the arene ring from Ar = Ph to 1,3-Me_2Ph has virtually no effect on the acceptor properties of the arene. Instead, these ligand modifications do have a considerable effect on the donating ability of the C_6 ring, the origin of which was delineated in Chapter 3. This is confirmed by the increase in backdonation to the CO ligands in **Vc** compared to **Vb**, and concurs with the observed/calculated CO stretching frequencies (*vide supra*).

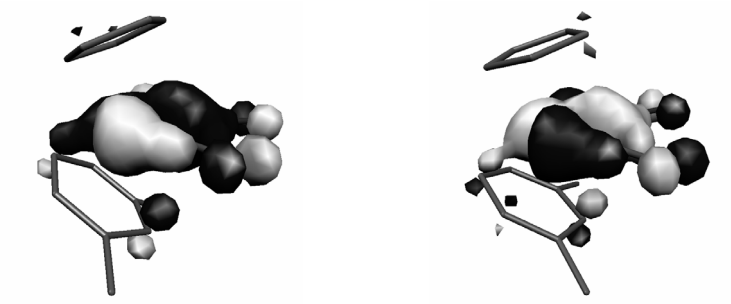

	Vb	**Vc**
L = arene	0.119	0.122
L = $(CO)_2$	0.216	0.242

Figure 4.4. Representation of the HOMO in **Vb**/**c**, and its contribution (e) to Ti→L backdonation for L = arene and $(CO)_2$.

4.3. CONCLUSIONS

The synthesis and characterisation of a series of *ansa*-Cp-arene titanium(II) cations shows that low-valent species of this type are accessible, lending credence to the Ti(II)/Ti(IV) redox mechanism that is proposed for catalytic ethylene trimerisation by these compounds. The coordination of the pendant arene moiety allows for stabilisation of the low-valent metal centre by π-backdonation into the arene π^*-system. Modifications in the Cp-arene ligand architecture are most prominently reflected in the electron-donation

capacity of the pendant arene moiety, whereas the acceptor properties appear to be less sensitive. This may, however, be due to the presence of the strong π-accepting CO ligands that compete for backdonation from the metal centre. The strain induced by the *ansa*-Cp-arene coordination prevents full reduction of the arene ring and this renders the switching between the Ti(II) and Ti(IV) states in the catalytic cycle reversible.

4.4. Experimental Section

General Considerations. For experimental details, see the Experimental Section in Chapter 2. In addition: CO (Praxair, 4.7 LBX) was used as received. IR spectra were recorded on an Interspec 301-X spectrometer inside a glovebox. Samples were prepared as films on KBr plates by evaporation of a solution of the compound, or as nujol mulls between KBr plates.

Attempted synthesis of [Ar-CMe$_2$-η^5-C$_5$H$_4$]Ti(2,3-dimethyl-1,3-butadiene)R (R = Cl, Me). A solution of [Ar-CMe$_2$-η^5-C$_5$H$_4$]TiCl$_3$ (**2b**, 172 mg, 0.47 mmol) in 10 mL of THF was cooled to -80 ºC and 1 equiv of (C$_6$H$_{10}$)Mg(THF)$_2$ (123 mg, 0.49 mmol) was added as a solid. The mixture quickly became darker, and slow warming to -50 ºC resulted in a dark green colour. Upon warming to 0 ºC, the solution became dark red, and stirring was continued at 0 ºC for 2 hours. The solvent was removed *in vacuo*, and the product extracted into hexane. Evaporation of all volatiles afforded a black tar, which was analysed by ^{1}H NMR to contain the desired species [Ar-CMe$_2$-η^5-C$_5$H$_4$]Ti(2,3-dimethyl-1,3-butadiene)Cl. ^{1}H NMR (400 MHz, C$_6$D$_6$, 25 ºC) δ 7.62 (s, 2H, Ar *o*-H), 6.69 (s, 1H, Ar *p*-H), 6.21 (ps t, *J* = 2.3, 2H, Cp), 5.31 (ps t, *J* = 2.3, 2H, Cp), 2.83 (d, *J* = 8.6, 2H, TiC*H*H'), 2.15 (s, 6H, ArMe), 1.89 (s, 6H, diene-Me), 1.76 (s, 6H, CMe$_2$), 1.48 (d, *J* = 8.6, 2H, TiCH*H*').

The same reaction, but with [Ar-CMe$_2$-η^5-C$_5$H$_4$]TiCl$_2$Me (obtained from the reaction of **2b** with AlMe$_3$, as described for Cp*TiCl$_2$Me)[71] gave a similar black product. ^{1}H NMR (400 MHz, C$_6$D$_6$, 25 ºC) δ 7.06 (s, 2H, Ar *o*-H), 6.72 (s, 1H, Ar *p*-H), 6.11 (ps t, *J* = 2.5, Cp), 5.48 (ps t, *J* = 2.5, Cp), 2.82 (d, *J* = 8.4, 2H, TiC*H*H'), 2.17 (s, 6H, ArMe), 1.95 (s, 6H, diene-Me), 0.99 (d, *J* = 8.4, TiCH*H*'), -0.05 (s, 3H, TiMe).

{[η^6-Ar-CMe$_2$-η^5-C$_5$H$_4$]Ti(CO)$_2$}[B(C$_6$F$_5$)$_4$] (5b). A powdered sample of solid **3b** (103 mg, 106 μmol) was pressurised with 1 bar of CO. After standing at room temperature for 3 days, the orange colour of the starting material darkened to red-brown. The excess CO was pumped off and the residue washed with 5 mL of cold (-30 ºC) bromobenzene. Subsequent washing with pentane and drying *in vacuo* gave 87 mg of **5b** as a red powder (87.5 μmol, 82%). Crystals suitable for X-ray analysis were obtained by diffusion of cyclohexane into a bromobenzene solution of **5b**. ^{1}H NMR (500 MHz, C$_6$D$_5$Br, 25 ºC) δ 5.00 (s, 1H, Ar *p*-H), 4.95 (s, 2H, Cp), 4.38 (s, 2H, Ar *o*-H), 3.91 (s, 2H, Cp), 1.69 (s, 6H, Ar Me), 0.69 (s, 6H, CMe$_2$). ^{13}C NMR for the cationic part (125.7 MHz, C$_6$D$_5$Br, 25 ºC) δ 227.3 (s, CO), 136.4 (s, Ar *m*-C), 104.8 (d, *J* = 180, Cp CH), 102.6 (d, *J* = 173, Ar *o*-CH), 100.3 (d, *J* = 175, Ar *p*-CH), 91.3 (s, Cp *ipso*-C), 86.8 (s, Ar *ipso*-C), 83.4 (d, *J* = 181, Cp CH), 38.7 (s, *C*Me$_2$),

21.3 (q, J = 129, Ar Me), 19.5 (q, J = 127, C*Me*$_2$). IR (ν, cm^{-1}), film from C_6D_5Br on KBr plates: 2055, 2022 (CO); nujol mull: 2052, 2023 (CO). Anal. Calcd for $C_{42}H_{19}BF_{20}O_2Ti$: C, 50.74; H, 1.93. Found: C, 50.58 ; H, 2.00.

Identification of acetone as a product from the reaction of 3b with CO. An NMR tube containing solid **3b** was degassed on a high-vacuum line and backfilled with 1 bar of CO. After standing at room temperature for 4 days, the color of the solid had turned reddish. The tube was frozen in liquid N_2, the valve opened under N_2 flow, and 0.5 mL of wet C_6D_5Br was added with a pipette. The tube was closed and allowed to warm to room temperature. The ^{1}H NMR spectrum showed signals for **5b**, a broad signal attributed to H_2O, and acetone (δ 1.81 ppm). The peaks for **5b** slowly disappeared in the course of several hours. In a control experiment, a dried (empty) tube was frozen in liquid N_2, and under N_2 flow 0.5 mL of C_6D_5Br was added. ^{1}H NMR spectroscopy showed only residual solvent peaks and some H_2O, showing that the acetone observed is not due to adventitious traces, but stems from the reaction.

General procedure for NMR tube scale carbonylation of 3a-f and 3h. A C_6D_5Br solution of the appropriate titanium dimethyl cation (**3a-f** or **3h**), either isolated or prepared *in situ* from **2a-f** or **2h** and $[Ph_3C][B(C_6F_5)_4]$, was degassed on a high-vacuum line by three freeze-pump-thaw cycles. The tube was backfilled with 1 bar of CO and the reaction was monitored by ^{1}H NMR. When all starting material was consumed (< 30 min for compounds with C_1 bridge, several hours for C_2-bridged compounds), the excess CO was pumped off. Samples for IR spectroscopy were prepared in the glovebox. A drop of the solution was taken from the NMR tube and placed on top of a KBr plate. The solvent was pumped off, leaving a red film on the plate, which was placed immediately in the FTIR spectrometer in the glovebox and the IR spectrum was recorded.

{[η^6-Ph-CMe$_2$-η^5-C$_5$H$_4$]Ti(CO)$_2$}[B(C$_6$F$_5$)$_4$] (5a). ^{1}H NMR (500 MHz, C_6D_5Br, 25 ºC) δ 5.91 (t, J = 7.3, 2H, Ph *m*-H), 5.27 (t, J = 7.1, 1H, Ph *p*-H), 5.01 (ps t, 2H, Cp), 4.28 (d, J = 7.6, Ph *o*-H), 3.89 (ps t, 2H, Cp), 0.62 (s, 6H, CMe$_2$). ^{13}C NMR for the cationic part (125.7 MHz, C_6D_5Br, 25 ºC) δ 226.6 (CO), 121.5 (Ph *m*-CH), 105.2 (Cp CH), 105.1 (Ph *o*-CH), 94.5 (Ph *p*-CH), 90.6 (Ph *ipso*-C), 87.8 (Cp *ipso*-C), 83.0 (Cp CH), 38.8 (*C*Me$_2$), 19.1 (C*Me*$_2$). IR (ν, cm^{-1}), film from C_6D_5Br on KBr plates: 2064, 2032 (CO).

{[η^6-Ar-CH$_2$CMe$_2$-η^5-C$_5$H$_4$]Ti(CO)$_2$}[B(C$_6$F$_5$)$_4$] (5c). ^{1}H NMR (500 MHz, C_6D_5Br, 25 ºC) δ 5.37 (s, 2H, Ar *o*-H), 5.15 (s, 2H, Cp), 4.78 (s, 2H, Cp), 4.62 (s, 1H, Ar *p*-H), 2.15 (s, 2H, CH_2), 1.72 (s, 6H, ArMe), 0.87 (s, 6H, CMe$_2$). ^{13}C NMR for the cationic part (125.7 MHz, C_6D_5Br, 25 ºC) δ 237.0 (CO), 137.0 (Cp *ipso*-C), 129.0 (Ar *m*-C), 128.4 (Ar *ipso*-C), 110.3 (Ar *o*-CH), 105.0 (Ar *p*-CH), 97.1 (Cp CH), 93.3 (Cp CH), 50.8 (CH_2), 39.4 (*C*Me$_2$), 30.0 (C*Me*$_2$), 21.0 (ArMe). IR (ν, cm^{-1}), film from C_6D_5Br on KBr plates: 2039, 1997 (CO).

{[η^6-Ph-CMe$_2$-η^5-C$_5$H$_3$SiMe$_3$]Ti(CO)$_2$}[B(C$_6$F$_5$)$_4$] (5d). ^{1}H NMR (500 MHz, C_6D_5Br, 25 ºC) δ 5.95 (t, J = 7.3, 1H, Ph *m*-H), 5.93 (t, J = 7.3, 1H, Ph *m*-H), 5.33 (t, J = 6.9, 1H, Ph *p*-H), 5.29 (s, 1H, Cp), 4.40 (overlapped d, 2H, Ph *o*-H), 4.33 (s, 1H, Cp), 4.18 (s, 1H, Cp), 0.72 (s, 3H, CMe$_2$), 0.64 (s, 3H, CMe$_2$), 0.10 (s, 9H, SiMe$_3$). ^{13}C NMR for the cationic part (approx. values taken from a HSQC spectrum; only CH resonances, C_6D_6, 25 ºC) δ 123 (Ph

m-CH), 120 (Ph *m*-CH), 113 (Cp CH), 106 (Ph *o*-CH), 104 (Ph *o*-CH), 95 (Ph *p*-CH), 89 (Cp CH), 88 (Cp CH), 20 (C*Me*$_2$), 19 (C*Me*$_2$), -1 (SiMe$_3$). ^{13}C NMR IR (ν, cm^{-1}), film from C_6D_5Br on KBr plates: 2056, 2022 (CO).

{[η^6-Ar-CH$_2$-η^5-C$_5$H$_3$SiMe$_3$]Ti(CO)$_2$}[B(C$_6$F$_5$)$_4$] (5e). ^{1}H NMR (500 MHz, C_6D_5Br, 25 ºC) δ 5.15 (s, 1H, Cp), 4.93 (s, 1H, Ar *p*-H), 4.27 (s, 1H, Cp), 4.15 (s, 1H, Ar *o*-H), 4.14 (s, 1H, Cp), 4.06 (s, 1H, Ar *o*-H), 2.50 (d, *J* = 12.7, 1H, CH$_2$), 2.32 (d, *J* = 12.7, 1H, CH$_2$), 1.66 (s, 3H, ArMe), 1.65 (s, 3H, ArMe), 0.07 (s, 9H, SiMe$_3$). ^{13}C NMR for the cationic part (125.7 MHz, C_6D_5Br, 25 ºC) δ 232.0 (CO), 227.8 (CO), 137.5 (Ar *m*-C), 135.8 (Ar *m*-C), 118.7 (Cp *C*SiMe$_3$), 111.7 (Cp CH), 106.0 (Ar *o*-CH), 105.3 (Ar *o*-CH), 100.8 (Ar *p*-CH), 90.9 (Cp CH), 90.3 (Cp CH), 83.4 (Cp *ipso*-C), 78.3 (Ar *ipso*-C), 32.8 (CH$_2$), 21.2 (Ar Me), 21.0 (Ar Me), -1.4 (SiMe$_3$). IR (ν, cm^{-1}), film from C_6D_5Br on KBr plates: 2047, 2010 (CO).

{[η^6-Ar-CMe$_2$-η^5-C$_5$H$_3$SiMe$_3$]Ti(CO)$_2$}[B(C$_6$F$_5$)$_4$] (5f). ^{1}H NMR (500 MHz, C_6D_5Br, 25 ºC) δ 5.30 (s, 1H, Cp), 5.13 (s, 1H, Ar *p*-H), 4.49 (s, 1H, Ar *o*-H), 4.46 (s, 1H, Ar *o*-H), 4.41 (s, 1H, Cp), 4.35 (s, 1H, Cp), 1.81 (s, 3H, ArMe), 1.80 (s, 3H, ArMe), 0.86 (s, 3H, CMe$_2$), 0.79 (s, 3H, CMe$_2$), 0.17 (s, 9H, SiMe$_3$). ^{13}C NMR for the cationic part (125.7 MHz, C_6D_5Br, 25 ºC) δ 231.2 (CO), 227.1 (CO), 137.2 (Ar *m*-C), 135.3 (Ar *m*-C), 117.9 (Cp *C*SiMe$_3$), 111.6 (Cp CH), 102.8 (Ar *o*-CH), 101.9 (Ar *o*-CH), 100.8 (Ar *p*-CH), 91.8 (Cp *ipso*-C), 90.2 (Ar *ipso*-C), 88.9 (Cp CH), 88.0 (Cp CH), 38.7 (*C*Me$_2$), 21.4 (Ar Me), 21.2 (Ar Me), 19.9 (CMe$_2$), 19.3 (CMe$_2$), -1.35 (SiMe$_3$). IR (ν, cm^{-1}), film from C_6D_5Br on KBr plates: 2048, 2012 (CO).

{[η^6-Ar-CH$_2$CMe$_2$-η^6-C$_5$H$_3$SiMe$_3$]Ti(CO)$_2$}[B(C$_6$F$_5$)$_4$] (5h). ^{1}H NMR (500 MHz, C_6D_5Br, 25 ºC) δ 5.65 (s, 1H, Ar), 5.65 (s, 1H, Cp), 5.36 (s, 1H, Cp), 5.35 (s, 1H, Cp), 5.35 (s, 1H, Ar), 4.74 (s, 1H, Ar), 2.28 (s, 2H, CH$_2$), 1.84 (s, 3H, ArMe), 1.82 (s, 3H, ArMe), 0.99 (s, 3H, CMe$_2$), 0.98 (s, 3H, CMe$_2$), 0.15 (s, 9H, SiMe$_3$). ^{13}C NMR for the cationic part (125.7 MHz, C_6D_5Br, 25 ºC) δ 239.2 (CO), 237.4 (CO) 139.2 (Cp *ipso*-C), 131.5 (Ar *m*-C), 128.6 (Ar *ipso*-C), 125.4 (Ar *m*-C), 112.0 (Ar *o*-CH), 108.4 (Ar *o*-CH), 106.2 (Ar *p*-CH), 104.9 (Cp CH), 99.7 (Cp CH), 99.3 (Cp CH), 50.5 (CH$_2$), 39.3 (*C*Me$_2$), 32.0 (C*Me*$_2$), 28.2 (C*Me*$_2$), 21.4 (ArMe), 20.8 (ArMe), -0.9 (SiMe$_3$). IR (ν, cm^{-1}), film from C_6D_5Br on KBr plates: 2033, 1989 (CO).

X-ray crystal structure. A suitable crystal of **5b** was mounted on top of a glass fibre in a drybox and transferred, using inert-atmosphere handling techniques, into the cold nitrogen stream of a Bruker SMART APEX CCD diffractometer. The final unit cell was obtained from the xyz centroids of 8874 reflections after integration. Intensity data were corrected for Lorentz and polarisation effects, scale variation, for decay and absorption: a multiscan absorption correction was applied, based on the intensities of symmetry-related reflections measured at different angular settings (*SADABS)*.[72] The structure was solved by Patterson methods and extension of the model was accomplished by direct methods applied to difference structure factors using the program *DIRDIF*.[73] A difference Fourier synthesis resulted in the location of all hydrogen atoms and the hydrogen atom coordinates and isotropic displacement parameters were refined freely. The final difference Fourier map revealed features within the range -1.01 to +0.60(8) e/Å^3 located near the Br position of the

bromobenzene solvate molecule. All refinement and geometry calculations were performed with the program packages *SHELXL*[74] and *PLATON*.[75] Crystal data and details on data collection and refinement are presented in Table 4.8.

Table 4.8. Crystallographic data for **5b**.

chem formula	$[C_{18}H_{19}O_2Ti]^+[C_{24}BF_{20}]^-$ $\cdot C_6H_5Br$	F(000)	2280
M_r	1151.27	temp (K)	100(1)
cryst syst	monoclinic	θ range (º)	2.57–25.68
color, habit	red, needle	data collected (h,k,l)	-19:19, -21:21, -20:20
size (mm)	0.51 x 0.19 x 0.11	min and max transm	0.6196, 0.8760
space group	$P2_1/c$	no. of rflns collected	32715
a (Å)	15.902(2)	no. of indpndt reflns	8296
b (Å)	17.780(2)	observed reflns	5883 ($F_o \geq 4\,\sigma\,(F_o)$)
c (Å)	17.100(2)	R(F) (%)	4.95
β (º)	115.144(2)	$wR(F^2)$ (%)	12.61
V (Å^3)	4376.7(9)	GooF	1.036
Z	4	weighting a,b	0.0579, 3.5774
ρ_{calc}, g.cm^{-3}	1.747	params refined	754
μ(Mo K_α), cm^{-1}	12.36	min, max resid dens	-1.01, 0.60(8)

Computational Studies. The geometry optimisations and charge decomposition analyses were performed as described in Chapter 3. A frequency analysis of the optimised structures showed these to be minima on the potential energy surface, and afforded the calculated CO absorption frequencies.

4.5. REFERENCES

(1) Blok, A. N. J.; Budzelaar, P. H. M.; Gal, A. W. *Organometallics* **2003**, *22*, 2564.
(2) De Bruin, T. J. M.; Magna, L.; Raybaud, P.; Toulhoat, H. *Organometallics* **2003**, *22*, 3404.
(3) Tobisch, S.; Ziegler, T. *Organometallics* **2003**, *22*, 5392.
(4) Chirik, P. J.; Bouwkamp, M. W., *Complexes of Titanium in Oxidation States 0 to II*, in Comprehensive Organometallic Chemistry III, p243-279, Elsevier, **2007**.
(5) Chirik, P. J.; Bradley, C. A., *Complexes of Zirconium and Hafnium in Oxidation States 0 to II*, in Comprehensive Organometallic Chemistry III, p697-739, Elsevier, **2007**.
(6) Brintzinger, H.; Bercaw, J. E. *J. Am. Chem. Soc.* **1970**, *92*, 6182.
(7) Hitchcock, P. B.; Kerton, F. M.; Lawless, G. A. *J. Am. Chem. Soc.* **1998**, *120*, 10264.
(8) Horacek, M.; Kupfer, V.; Thewalt, U.; Stepnicka, P.; Polasek, M.; Mach, K. *Organometallics* **1999**, *18*, 3572.
(9) Pool, J. A.; Lobkovsky, E.; Chirik, P. J. *Nature* **2004**, *427*, 527.
(10) MacLachlan, E. A.; Fryzuk, M. D. *Organometallics* **2006**, *25*, 1530.
(11) Hanna, T. E.; Bernskoetter, W. H.; Bouwkamp, M. W.; Lobkovsky, E.; Chirik, P. J. *Organometallics* **2007**, *26*, 2431.
(12) Hanna, T. E.; Lobkovsky, E.; Chirik, P. J. *J. Am. Chem. Soc.* **2006**, *128*, 6018.
(13) Hessen, B.; Teuben, J. H. *J. Organomet. Chem.* **1988**, *358*, 135.
(14) Yamamoto, H.; Yasuda, H.; Tatsumi, K.; Lee, K.; Nakamura, A.; Chen, J.; Kai, Y.; Kasai, N. *Organometallics* **1989**, *8*, 105.
(15) Spencer, M. D.; Wilson, S. R.; Girolami, G. S. *Organometallics* **1997**, *16*, 3055.
(16) Beetstra, D. J.; Meetsma, A.; Hessen, B.; Teuben, J. H. *Organometallics* **2003**, *22*, 4372.
(17) Stein, B. K.; Frerichs, S. R.; Ellis, J. E. *Organometallics* **1987**, *6*, 2017.
(18) Wielstra, Y.; Gambarotta, S.; Roedelof, J. B.; Chiang, M. Y. *Organometallics* **1988**, *7*, 2177.
(19) You, Y.; Wilson, S. R.; Girolami, G. S. *Organometallics* **1994**, *13*, 4655.
(20) Edema, J. J. H.; Duchateau, R.; Gambarotta, S.; Hynes, R.; Gabe, E. *Inorg. Chem.* **1991**, *30*, 154.
(21) Araya, M. A.; Cotton, F. A.; Matonic, J. H.; Murillo, C. A. *Inorg. Chem.* **1995**, *34*, 5424.
(22) Jensen, J. A.; Wilson, S. R.; Schultz, A. J.; Girolami, G. S. *J. Am. Chem. Soc.* **1987**, *109*, 8094.
(23) Sikora, D. J.; Macomber, D. W.; Rausch, M. D. *Adv. Organomet. Chem.* **1986**, *25*, 317.
(24) Rosenthal, U.; Burlakov, V. V.; Arndt, P.; Baumann, W.; Spannenberg, A. *Organometallics* **2003**, *22*, 884.
(25) Sikora, D. J.; Macomber, D. W.; Rausch, M. D. *Adv. Organomet. Chem.* **1986**, *25*, 317.
(26) Brintzinger, H.; Marvich, R. H. *J. Am. Chem. Soc.* **1971**, *93*, 2046.
(27) Bercaw, J. E.; Marvich, R. H.; Bell, L. G.; Brintzinger, H. H. *J. Am. Chem. Soc.* **1972**, *94*, 1219.
(28) Fachinetti, G.; Floriani, C. *J. Chem. Soc., Chem. Commun.* **1972**, 654.
(29) Fachinetti, G.; Floriani, C. *J. Organomet. Chem.* **1974**, *71*, C5-C7.
(30) Smith, J. A.; Brintzinger, H. H. *J. Organomet. Chem.* **1981**, *218*, 159.
(31) Erker, G.; Dorf, U.; Czisch, P.; Peterson, J. L. *Organometallics* **1986**, *5*, 668.
(32) Deckers, P. J. W.; Van der Linden, A. J.; Meetsma, A.; Hessen, B. *Eur. J. Inorg. Chem.* **2000**, 929.
(33) Hagadorn, J. R.; Arnold, J. *Angew. Chem. Int. Ed.* **1998**, *37*, 1729.
(34) Ozerov, O. V.; Patrick, B. O.; Ladipo, F. T. *J. Am. Chem. Soc.* **2000**, *122*, 6423.
(35) Fryzuk, M. D.; Kozak, C. M.; Mehrkhodavandi, P.; Morello, L.; Patrick, B. O.; Rettig, S. J. *J. Am. Chem. Soc.* **2002**, *124*, 516.
(36) Kissounko, D.; Epshteyn, A.; Fettinger, J. C.; Sita, L. R. *Organometallics* **2006**, *25*, 531.
(37) Graham, T. W.; Kickham, J.; Courtenay, S.; Wei, P.; Stephan, D. W. *Organometallics* **2004**, *23*, 3309.
(38) Lee, H.; Bonanno, J. B.; Hascall, T.; Cordaro, J.; Hahn, J. M.; Parkin, G. *J. Chem. Soc., Dalton Trans.* **1999**, 1365.
(39) Kool, L. B.; Rausch, M. D.; Alt, H. G.; Herberhold, M.; Wolf, B.; Thewalt, U. *J. Organomet. Chem.* **1985**, *297*, 159.
(40) Kalodimos, C. G.; Gerothanassis, I. P.; Pierattelli, R.; Ancian, B. *Inorg. Chem.* **1999**, *38*, 4283.

(41) Antonelli, D.; Tjaden, E.; Stryker, J. *Organometallics* **1994**, *13*, 763.
(42) Lupinetti, A. J.; Strauss, S. H.; Frenking, G. *Progr. Inorg. Chem.,* **2001**, *49*, 1.
(43) Dias, H. V. R.; Fianchini, M. *Angew. Chem. Int. Ed.* **2007**, *46*, 2188.
(44) Brintzinger, H. H. *J. Organomet. Chem.* **1979**, *171*, 337.
(45) Marsella, J.; Curtis, C.; Bercaw, J.; Caulton, K. *J. Am. Chem. Soc.* **1980**, *102*, 7244.
(46) Procopio, L. J.; Carroll, P. J.; Berry, D. H. *Polyhedron* **1995**, *14*, 45.
(47) Howard, W. A.; Trnka, T. M.; Parkin, G. *Organometallics* **1995**, *14*, 4037.
(48) Howard, W. A.; Parkin, G.; Rheingold, A. L. *Polyhedron* **1995**, *14*, 25.
(49) Burckhardt, U.; Tilley, T. D. *J. Am. Chem. Soc.* **1999**, *121*, 6328.
(50) Guram, A. S.; Swenson, D. C.; Jordan, R. F. *J. Am. Chem. Soc.* **1992**, *114*, 8991.
(51) Guo, Z.; Swenson, D.; Guram, A.; Jordan, R. *Organometallics* **1994**, *13*, 766.
(52) Otten, E.; Meetsma, A.; Hessen, B. *J. Am. Chem. Soc.* **2007**, *129*, 10100.
(53) Sikora, D.; Rausch, M.; Rogers, R.; Atwood, J. *J. Am. Chem. Soc.* **1981**, *103*, 1265.
(54) Cuenca, T.; Gomez, R.; Gomez-Sal, P.; Royo, P. *J. Organomet. Chem.* **1993**, *454*, 105.
(55) Van Raaij, E. U.; Schmulbach, C. D.; Brintzinger, H. H. *J. Organomet. Chem.* **1987**, *328*, 275.
(56) Brackemeyer, T.; Erker, G.; Frohlich, R. *Organometallics* **1997**, *16*, 531.
(57) Pampaloni, G.; Tripepi, G. *J. Organomet. Chem.* **2000**, *593-594*, 19.
(58) Calderazzo, F.; Pampaloni, G.; Tripepi, G. *Organometallics* **1997**, *16*, 4943.
(59) Zachmanoglou, C. E.; Docrat, A.; Bridgewater, B. M.; Parkin, G.; Brandow, C. G.; Bercaw, J. E.; Jardine, C. N.; Lyall, M.; Green, J. C.; Keister, J. B. *J. Am. Chem. Soc.* **2002**, *124*, 9525.
(60) Jang, J. H.; Lee, J. G.; Lee, H.; Xie, Y.; Schaefer, H. F. *J. Phys. Chem. A* **1998**, *102*, 5298.
(61) Koch, W.; Holthausen, M. C. *A Chemist's Guide to Density Functional Theory*; Wiley-VCH, Weinheim: **2002**; pp 130-136.
(62) Lauher, J. W.; Hoffmann, R. *J. Am. Chem. Soc.* **1976**, *98*, 1729.
(63) Casarin, M.; Ciliberto, E.; Gulino, A.; Fragala, I. *Organometallics* **1989**, *8*, 900.
(64) Dewar, J. S. *Bull. Soc. Chim. Fr.* **1951**, *18*, C71-C79.
(65) Chatt, J.; Duncanson, L. A. *J. Chem. Soc.* **1953**, 2939.
(66) Dapprich, S.; Frenking, G. *J. Phys. Chem.* **1995**, *99*, 9352.
(67) Frenking, G.; Pidun, U. *J. Chem. Soc., Dalton Trans* **1997**, 1653.
(68) Szilagyi, R. K.; Frenking, G. *Organometallics* **1997**, *16*, 4807.
(69) Diefenbach, A.; Bickelhaupt, F. M.; Frenking, G. *J. Am. Chem. Soc.* **2000**, *122*, 6449.
(70) Decker, S. A.; Klobukowski, M. *J. Am. Chem. Soc.* **1998**, *120*, 9342.
(71) Martin, A.; Mena, M.; Pellinghelli, M. A.; Royo, P.; Serrano, R.; Tiripicchio, A. *J. Chem. Soc. Dalton Trans.* **1993**, 2117.
(72) Sheldrick, G. M., *SADABS.* Version 2.10. *Multi-Scan Absorption Correction Program*. University of Göttingen, Germany, **2006**.
(73) Beurskens, P. T.; Beurskens, G.; De Gelder, R.; García-Granda, S.; Gould, R. O.; Israël, R.; Smits, J. M. M., *The DIRDIF-99 Program System,* Crystallography Laboratory, Univeristy of Nijmegen, The Netherlands, **1999**.
(74) Sheldrick, G. M., *SHELXL-97. Program for the Refinement of Crystal Structures.* University of Göttingen, Germany, **1997**.
(75) Spek, A. L., *PLATON. Program for the Automated Analysis of Molecular Geometry (A Multipurpose Crystallographic Tool).* Version of Aug. 2006. University of Utrecht, The Netherlands, *J. Appl. Crystallogr.* **2003**, *36*, 7.